

Critical Role of Filamin-binding LIM Protein 1 (FBLP-1)/Migfilin in Regulation of Bone Remodeling*

Received for publication, December 6, 2011, and in revised form, April 5, 2012. Published, JBC Papers in Press, May 3, 2012, DOI 10.1074/jbc.M111.331249

Guozhi Xiao^{‡§1,2}, Hongqiang Cheng^{¶1,3}, Huiling Cao^{‡1}, Ka Chen^{||}, Yizeng Tu^{||}, Shibing Yu[‡], Hongli Jiao^{‡§}, Shengyong Yang[‡], Hee-Jeong Im[§], Di Chen[§], Ju Chen^{¶4}, and Chuanyue Wu^{||5}

From the [‡]Department of Medicine, University of Pittsburgh, Pittsburgh, Pennsylvania 15240, the [§]Department of Biochemistry, Rush University Medical Center, Chicago, Illinois 60612, the [¶]Department of Medicine, University of California San Diego, La Jolla, California 92093, and the ^{||}Department of Pathology, University of Pittsburgh, Pittsburgh, Pennsylvania 15261

Background: Bone remodeling must be precisely controlled to maintain a healthy bone mass.

Results: Knock-out of FBLP-1/migfilin causes a severe osteopenic phenotype in mice.

Conclusion: FBLP-1/migfilin regulates bone remodeling through modulating both osteoblast behavior and osteoclast differentiation.

Significance: Identifying molecules that regulate bone remodeling is critical for understanding the pathogenesis of bone diseases and developing novel therapeutic approaches.

Bone remodeling is a complex process that must be precisely controlled to maintain a healthy life. We show here that filamin-binding LIM protein 1 (FBLP-1, also known as migfilin), a kindlin- and filamin-binding focal adhesion protein, is essential for proper control of bone remodeling. Genetic inactivation of *FBLIM1* (the gene encoding FBLP-1) in mice resulted in a severe osteopenic phenotype. Primary FBLP-1 null bone marrow stromal cells (BMSCs) exhibited significantly reduced extracellular matrix adhesion and migration compared with wild type BMSCs. Loss of FBLP-1 significantly impaired the growth and survival of BMSCs *in vitro* and decreased the number of osteoblast (OB) progenitors in bone marrow and OB differentiation *in vivo*. Furthermore, the loss of FBLP-1 caused a dramatic increase of osteoclast (OCL) differentiation *in vivo*. The level of receptor activator of nuclear factor κ B ligand (RANKL), a key regulator of OCL differentiation, was markedly increased in FBLP-1 null BMSCs. The capacity of FBLP-1 null bone marrow monocytes (BMMs) to differentiate into multinucleated OCLs in response to exogenously supplied RANKL, however, was not different from that of WT BMMs. Finally, we show that a loss of FBLP-1 promotes activating phosphorylation of ERK1/2. Inhibition of ERK1/2 activation substantially suppressed the increase of RANKL induced by the loss of FBLP-1. Our results identify FBLP-1 as a key regulator of bone homeostasis and suggest that FBLP-1 functions in this process through modulat-

ing both the intrinsic properties of OB/BMSCs (*i.e.*, BMSC-extracellular matrix adhesion and migration, cell growth, survival, and differentiation) and the communication between OB/BMSCs and BMMs (*i.e.*, RANKL expression) that controls osteoclastogenesis.

Bone remodeling is a dynamic process whose balance is maintained through precise control of two functionally opposing events, namely bone formation and resorption. Imbalance of bone formation and resorption is a causal factor of many human metabolic bone diseases including osteoporosis. At the cellular level, bone formation is controlled by osteoblasts (OBs),⁶ a population of bone matrix-producing cells derived from BMSCs. The behavior of BMSCs (*e.g.*, ECM adhesion and migration) therefore exerts profound effects on bone formation. Bone resorption, on the other hand, is mediated by OCLs, which originate from the bone marrow monocyte (BMM)/macrophage lineage (1). The formation and maturation of OCLs are closely regulated by factors produced by OBs/BMSCs such as RANKL, a member of the TNF cytokine family, and osteoprotegerin (OPG), a soluble decoy receptor that blocks RANKL binding to RANK and thereby inhibits OCL differentiation (2–5). During early OCL differentiation, RANKL binds to its receptor RANK on OCL precursors and recruits TRAF6, resulting in activation of multiple signaling pathways involving IKK, NF- κ B, MAPKs (p38, ERK, and JNK), and AKT (6–9). Activation of MAPKs leads to activation and nuclear translocation of transcription factor NFATc1 (8), a master regulator of OCL differentiation and bone resorption.

Whereas bone formation and resorption are dynamic processes that are executed through actions of different cell popu-

* This work was supported, in whole or in part, by National Institutes of Health Grants AR059647 (to G. X.) and GM65188 (to C. W.).

¹ These authors contributed equally to this work.

² To whom correspondence may be addressed: Cohn Research Bldg., Rm. 518, Rush University Medical Center, 1735 West Harrison St., Chicago, IL 60612. Tel.: 312-942-4879; E-mail: xiaogz118@gmail.com.

³ Present address: Program in Molecular Cell Biology, Dept. of Basic Medical Sciences, Zhejiang University School of Medicine, Hangzhou, China, 310058.

⁴ To whom correspondence may be addressed: Dept. of Medicine, University of California San Diego, 9500 Gilman Dr., La Jolla, CA 92093. E-mail: juichen@ucsd.edu.

⁵ To whom correspondence may be addressed: 707B Scaife Hall, Dept. of Pathology, University of Pittsburgh, 3550 Terrace St., Pittsburgh, PA 15261. Tel.: 412-648-2350; E-mail: carywu@pitt.edu.

⁶ The abbreviations used are: OB, osteoblast; BMSC, bone marrow stromal cell; ECM, extracellular matrix; OCL, osteoclast; RANKL, receptor activator of nuclear factor κ B ligand; BMM, bone marrow monocyte; CFU-F, colony forming unit-fibroblast; CFU-OB, colony forming unit-OB; Osx (+) Ob.nb/BPm, Osx-positive cells on trabecular bone surfaces counted and normalized to trabecular bone perimeter; TRAP, tartrate-resistant acid phosphatase; MBP, maltose-binding protein.

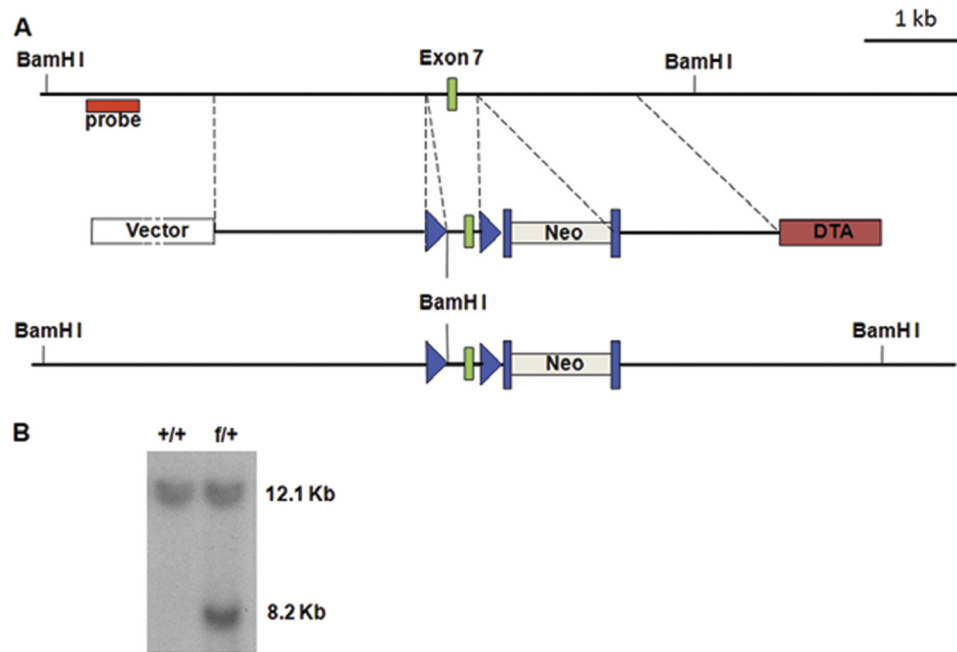


FIGURE 1. **Generation of *FBLIM1*^{-/-} mice.** *A*, genomic region of interest for *FBLIM1* is shown on the top. The middle is the targeting construct for *FBLIM1* where the exon 7 (green box) is floxed by two *LoxP* sites (blue triangles, center). A neomycin cassette (*Neo*) flanked by two *FRT* sites (blue rectangles) is inserted into the seventh intron. *DTA*, diphtheria toxic A chain gene; *Neo*, neomycin resistance gene. The floxed locus for *FBLIM1* after homologous recombination is shown at the bottom. *B*, DNA from *Neo*-positive ES cells was digested with restriction enzyme *Bam*HI and analyzed by Southern blot for WT (+/+, 12.1 kb) and targeted (f/+, 8.2 kb) alleles with probe as shown in *A* (red rectangle).

lations (*i.e.*, OB/BMSC and OCL), there is intimate communication between these cell populations, which is essential for orchestrating the balance of bone formation and resorption (10–14). This is illustrated by the fact that RANKL is synthesized primarily by OBs/BMSCs. Thus, OBs/BMSCs not only are responsible for bone formation but also play an important role in regulation of bone resorption via control of the expression of key OCL differentiation factors such as RANKL. Despite the importance, factors that control RANKL expression in OBs/BMSCs are incompletely understood.

FBLP-1 (also known as migfilin or Mig2-interacting protein) is a multidomain adaptor protein that we identified in a search for binding partners of kindlin-2 (also known as mitogen-inducible gene-2 or Mig-2) (15), which binds directly to integrins and regulates integrin signaling (16–20). Subsequently, we have found that FBLP-1 interacts with several important actin cytoskeletal and signaling proteins including filamin (15, 21, 22). Although *in vitro* studies using cultured cells and/or purified proteins have pointed to a role of FBLP-1 in regulation of cell-ECM adhesion, migration, cytoskeletal organization, and intracellular signaling (15, 21–29), the functions of FBLP-1 in tissues and organs were not known. To address this question, we have inactivated *FBLIM1* (the gene encoding FBLP-1) in mice and determined the functional consequences. Our studies reveal, for the first time, that FBLP-1 is critical for maintenance of bone homeostasis. Using primary BMSCs derived from FBLP-1 KO mice, we show that FBLP-1 is required for proper BMSC-ECM adhesion and migration. Furthermore, we have found that FBLP-1 is critical for control of OCL differentiation *in vivo*. Finally, we provide evidence suggesting that FBLP-1 functions in this process through regulation of signaling events in OBs/BMSCs that control RANKL expression rather than

altering intrinsically the differentiation potential of OCL precursors.

EXPERIMENTAL PROCEDURES

Generation of Monoclonal Antibodies Recognizing Mouse FBLP-1—Monoclonal antibodies recognizing mouse FBLP-1 were prepared using a GST fusion protein containing mouse FBLP-1 residues 1–222 as an antigen based on a previously described method (15). Hybridomas were initially screened for anti-FBLP-1 activity by ELISA using an MBP fusion protein containing mouse FBLP-1 residues 1–222. Mouse monoclonal antibodies recognizing MBP-FBLP-1 in ELISA were further tested by Western blotting using human HEK 293 cells overexpressing GFP-tagged mouse FBLP-1. Monoclonal antibody (clone 43.9) recognizing MBP- and GFP-tagged mouse FBLP-1 was selected and used in subsequent experiments.

Generation of *FBLIM1*^{-/-} Mice—Mouse FBLP-1 genomic DNA amplified from mouse embryonic stem cells (129/SvJ) was used to generate a *FBLIM1* targeting construct (Fig. 1A) following a protocol that we described (30). Specifically, one *LoxP* site was inserted into intron 6, and a second *LoxP* site together with a neomycin (*Neo*) cassette flanked by two *FRT* sites were inserted into intron 7. *DTA* cassette was used to assist homologous recombination. The targeting vector was linearized with restriction enzyme *Not*I and electroporated into R1 embryonic stem cells derived from 129/SvJ mice. Homologous recombinants were identified by Southern blotting. Genomic DNA from neo-positive cells was digested with restriction enzyme *Bam*HI and hybridized with the radiolabeled 5'-probe as indicated in Fig. 1A. The WT allele is represented as a 12.1-kb band, whereas an 8.2-kb band represents the targeted allele (Fig. 1B). Two independent homologous recombinant ES cell clones

FBLP-1 in Bone Remodeling

TABLE 1
DNA sequences of real time PCR primers

Name	5' primer	3' primer
<i>GAPDH</i>	CAGTGCCAGCCTCGTCCCCTAGA	CTGCAAATGGCAGCCCTGGTGAC
<i>Opg</i>	GGCTGAGTGTTTTGGTGGACAG	GCTGGAAGGTTTGCTCTTGTA
<i>Rankl</i>	GCCGAGGAAGGGAGAGAACG	CCCATCTCCTCCGAGCTGC

were microinjected into C57BL/6 blastocysts. Male chimeras were bred with female Black Swiss mice (Taconic Inc., Hudson, NY) to generate germ line-transmitted heterozygous mice carrying neo cassette (*FBLIMI^{fneo/+}*), which were confirmed by PCR of mouse tail DNA following a protocol that we described (31). To generate *FBLIMI^{-/-}* mice, we crossed the *FBLIMI^{fneo/+}* mice with Protamine-Cre mice (32), resulting in mice that were doubly heterozygous (*Pro-Cre; FBLIMI^{fneo/+}*). Cre expression in *Pro-Cre* mice is restricted to male germ cells undergoing spermatogenesis (32). Therefore *Pro-Cre; FBLIMI^{fneo/+}* males were crossed to female WT mice to generate germ line heterozygous null mutant offspring (+/-). Heterozygous mice were interbred to generate homozygous *FBLIMI^{-/-}* mice. Offspring were genotyped by PCR with following primer sets: WT allele primers (P1: 5'-AAT ACT CGT GGG TGG AGG TG-3' and P2: 5'-AAG CCT TTT GTG TGC CAA GT-3') and knock-out allele primers (Frtneo: 5'-AAT GGG CTG ACC GCT TCC TCG T-3' and P4: 5'-CAC AGC CTG GTT ATG TGG TG-3'). A loss of FBLP-1 in cells derived from *FBLIMI^{-/-}* but not WT control mice was confirmed by Western blotting with monoclonal antibody recognizing mouse FBLP-1 (see "Results").

Histological Evaluation, Bone Histomorphometry, and Immunohistochemistry—WT and *FBLIMI^{-/-}* mice were euthanized, and tibiae were fixed in 10% formalin at 4 °C for 24 h, decalcified in 10% EDTA (pH 7.4) for 10–14 days, and embedded in paraffin. Sections of tibiae from WT *FBLIMI^{-/-}* mice were used for TRAP staining as described previously (33). Bone histomorphometry such as OCL surface/bone surface and OCL number/bone perimeter in both primary and secondary spongiosa of tibiae was measured using an Image Pro Plus 6.2 software (Media Cybernetics, Inc.) as previously described (33). Five- μ m sections of tibiae were immunohistochemically stained with an antibody against RANKL (Santa Cruz, sc-9073), *Osx* (Abcam Inc., ab22552), or control IgG using the EnVision⁺ System-HRP (3,3'-diaminobenzidine tetrahydrochloride) kit (Dako North America, Inc.) as described previously (34). Fixed nondemineralized femurs were used for microcomputerized tomography analysis at the Center for Bone Biology using a VIVACT40 (SCANCO Medical AG) as previously described (34).

Quantitative RT-PCR—RNA isolation and reverse transcription were previously described (35). Quantitative real time RT-PCR analysis was performed to measure the relative mRNA levels using SYBR Green kit (Bio-Rad). The samples were normalized to *GAPDH* expression. The DNA sequences of primers used for real time PCR were summarized in Table 1.

Immunofluorescent Staining—Immunofluorescent staining was performed as we described (15). Briefly, BMSCs isolated from WT and *FBLIMI^{-/-}* mice were plated on type I collagen-coated coverslips and incubated in a 37 °C incubator under a 5%

CO₂, 95% air atmosphere for 20 h. At the end of incubation, the cells were fixed with 3.7% paraformaldehyde in PBS and permeabilized with 0.1% Triton X-100 in PBS. The cells were then dually stained with rhodamine-phalloidin and mouse monoclonal anti-FBLP-1 antibody 43.9, and the latter was detected with CY2-conjugated anti-mouse IgG antibodies.

Western Blot Analysis—Western blot analysis was performed as previously described (35, 36). Primary antibody against RANKL and secondary anti-rabbit or anti-mouse IgG antibodies conjugated with horseradish peroxidase were from Santa Cruz Biotechnology, Inc. Antibodies recognizing ERK1/2, phospho-ERK1/2 (Thr-202/Tyr-204), AKT, and phospho-AKT (Ser-473) were from Cell Signaling Technology, Inc. Mouse monoclonal antibody against β -actin was from Sigma-Aldrich.

Isolation of Primary BMSCs—Isolation of mouse primary BMSCs from WT and *FBLIMI^{-/-}* mice was described previously (37). Briefly, 6-week-old male WT and *FBLIMI^{-/-}* mice were euthanized. Femurs and tibiae were isolated, and the epiphyses were cut. Marrow was flushed with α -minimum essential medium (Invitrogen formula 01-0133D) containing 20% FBS and 1% penicillin/streptomycin into a 100-mm dish, and the cell suspension was aspirated up and down with a 20-gauge needle to break clumps of marrow. The cell suspension was then cultured in a T75 flask in the same medium. After 10 days, the cells reached confluence and were used for experiments.

Cell-ECM Adhesion Assay—Cell-ECM adhesion was analyzed using a quantitative centrifugal force assay based on a protocol that we previously described (38, 39). Briefly, primary BMSCs were isolated from WT and *FBLIMI^{-/-}* mice as we described (37). The cells (4×10^4 cells/well) were plated in triplicate in type I collagen- or fibronectin-coated 96-well plates. The plates were sealed with sealing films (USA Scientific) and centrifuged with a Sorvall RT7 Plus centrifuge equipped with a microplate carrier at 600 rpm, 4 °C for 3 min to facilitate cell settlement. The cells were observed under an Olympus IX70 microscope and recorded with a digital camera (four randomly selected fields in each well were photographed; >300 cells/field). The plates were incubated at 37 °C for 15 min and then inverted and centrifuged at 600 rpm, 37 °C for 5 min. After inverted centrifugation, the sealing films were removed, and the number of cells that remained was recorded again with the digital camera. Cell adhesion was calculated as the number of cells recorded after inverted centrifugation divided by the number of cells recorded before inverted centrifugation. The adhesion of *FBLIMI^{-/-}* BMSCs was compared with that of WT control BMSCs (normalized to 100%).

Cell Migration Assay—Cell migration was assessed by the ability of cells to migrate into a cell-free area in a scratch assay as we described (22, 40). Briefly, primary BMSCs from WT and

FBLIM1^{-/-} mice were cultured in dishes that were precoated with 10 μ g/ml fibronectin. The cell monolayers were wounded by scratching with a plastic pipette tip. After washing, the cells were incubated in α -minimum essential medium containing 2% FBS and 10 μ g/ml mitomycin C (to minimize cell proliferation) for 6.5 h. Images of five different segments of the cell-free area were recorded, and the distances traveled by the cells at the front in five different segments of the wound were measured. The distances traveled by *FBLIM1*^{-/-} BMSCs were compared with those of WT control BMSCs (normalized to 100%).

RNA Interference—Mouse MC4 cells, an OB-like cell line derived from MC3T3-E1 cells, were cultured in ascorbic acid-free α -minimum essential medium containing 10% FBS and 1% penicillin/streptomycin as we described (41). The siRNA that specifically targets mouse FBLP-1 transcript (target sequence: 5-GCATGGGAAGGAATTTCCACGAGAA-3) and a control siRNA that does not recognize any mouse transcripts were purchased from Invitrogen. The cells were transfected with the FBLP-1 or control siRNA with Lipofectamine 2000 (Invitrogen) following the manufacturer's protocols. Two days after siRNA transfection, the cells were analyzed by Western blotting and cell-ECM adhesion assays as described above.

Colony Forming Unit-Fibroblast (CFU-F) Assay and Colony Forming Unit-OB (CFU-OB) Assay—The CFU-F assay was performed for the expansion and enumeration of the mesenchymal stem cells from WT and *FBLIM1*^{-/-} bone marrow using the Mesencult Proliferation Kit (Mouse) according to the manufacturer's instruction (Stemcell Technologies, catalog number 05511). 1×10^6 bone marrow nucleated cells from WT and *FBLIM1*^{-/-} mice were seeded in 35-mm culture dishes and cultured for 10 days, and the numbers of CFU-Fs were counted under a microscope. For the CFU-OB assay, 1×10^6 bone marrow nucleated cells from WT and *FBLIM1*^{-/-} mice were seeded in 60-mm culture dishes in OB differentiation medium (complete α -minimum essential medium containing 50 μ g/ml L-ascorbic acid and 2.0 mM β -glycerophosphate). The media were changed every 2 days. At day 21, alizarin red staining was used to identify and enumerate the colonies containing mineralized bone matrix, which were designated CFU-OB colonies.

MTS Assay and TUNEL Staining—MTS assay was used to measure cell growth as described previously (42). Briefly, the cells were planted in a 96-well plate (1×10^4 cells/well) in 100 μ l of proliferation medium. The cells were incubated at 37 $^{\circ}$ C for 24 h to allow attachment. The medium was changed every 48 h. At different time points, 20 μ l of CellTitre96AQ solution reagent (Promega, Madison, WI) was added into each well and incubated for 2 h. The absorbance was recorded at 490 nm using a 96-well plate reader. Apoptosis of WT and *FBLIM1*^{-/-} BMSCs was evaluated by TUNEL staining using the ApopTag peroxidase *in situ* apoptosis detection kit according to the manufacturer's instructions (Millipore) as previously described (42). This method examines apoptosis by detection of DNA fragmentation. The DNA is detected by enzyme labeling of the free 3'-OH termini with modified nucleotides. These ends are localized in identifiable nuclei and apoptotic bodies.

Statistical Analysis—The data were analyzed with a GraphPad Prism software (4.0). One-way analysis of variance analysis was used followed by the Tukey test. The results were expressed as the means \pm S.D. Differences with a $p < 0.05$ were considered statistically significant.

RESULTS

FBLP-1 Deficiency Results in Severe Osteopenic Phenotype in Mice—To determine the functions of FBLP-1 *in vivo*, we inactivated *FBLIM1* in mice as described under "Experimental Procedures" (Fig. 1). *FBLIM1*^{-/-} mice were born with a normal Mendelian frequency, were fertile, and showed normal viability. However, comparison of bones from *FBLIM1*^{-/-} mice with WT controls revealed a severe osteopenic phenotype. Quantitative microcomputerized tomography analysis of femur histomorphometric parameters showed that *FBLIM1*^{-/-} mice had a significant reduction in bone volume/tissue volume and trabecular number and a marked increase in trabecular space compared with the WT littermates (Fig. 2). FBLP-1 deficiency decreased bone volume/tissue volume by 51% ($p = 0.0036$, WT versus KO), trabecular number by 34% ($p = 0.00028$, WT versus KO), and increased trabecular space by 53% ($p = 0.031$, WT versus KO).

Loss of FBLP-1 Compromises BMSC-ECM Adhesion and Migration—The osteopenic bone phenotype that we observed in *FBLIM1*^{-/-} mice prompted us to test the effects of FBLP-1 deficiency on cellular behavior of BMSCs, which are known to be critical for bone remodeling. FBLP-1 was detected by Western blotting in primary BMSCs isolated from WT control mice (Fig. 3E, WT) but not in those from *FBLIM1*^{-/-} mice (Fig. 3E, KO). Consistent with this, in WT but not *FBLIM1*^{-/-} BMSCs, clusters of FBLP-1 were detected at focal adhesions to which actin stress fibers were anchored (Fig. 3, A–D). Analyses of cell-ECM adhesion using a quantitative centrifugal force assay showed that elimination of FBLP-1 significantly reduced BMSC adhesion to type I collagen (Fig. 3F) and fibronectin (Fig. 3G), both of which are key ECM components in bone (43–47).

To confirm a role of FBLP-1 in regulation of ECM adhesion, we knocked down FBLP-1 from MC4 cells, an OB-like cell line derived from MC3T3-E1 cells (41), by RNAi (Fig. 3H). Consistent with the results obtained with *FBLIM1*^{-/-} BMSCs, knockdown of FBLP-1 significantly reduced MC4 cell-ECM adhesion (Fig. 3I).

We next tested whether FBLP-1 plays a role in regulation of BMSC migration. To do this, we compared migration of *FBLIM1*^{-/-} BMSCs with that of WT BMSCs. The results showed that a loss of FBLP-1 significantly compromised BMSC migration (Fig. 3J). Collectively, these results demonstrate an important role for FBLP-1 in regulation of BMSC behavior *in vitro*.

Loss of FBLP-1 Significantly Compromises Primary BMSC Growth and Survival, Decreases Number of OB Progenitors in Bone Marrow, and Inhibits OB Differentiation in Vivo—To investigate the effect of FBLP-1 ablation on the development of mesenchymal cells, we performed the CFU-F assays using bone marrow cells from both genotypes. The results showed that inactivation of the *FBLIM1* gene did not markedly alter the number of CFU-Fs in bone marrow (Fig. 4, A and B), suggesting

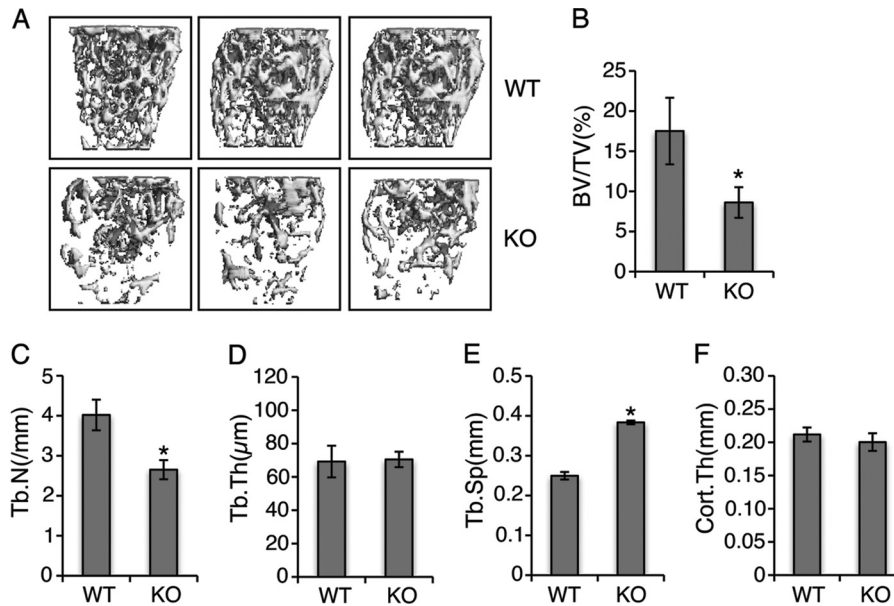


FIGURE 2. Inactivation of *FBLIM1* results in a severe osteopenic phenotype in mice. *A*, three-dimensional reconstruction from microcomputerized tomography scan of femurs from 3-month-old male *FBLIM1*^{-/-} mice and their WT male littermates. *B–F*, quantitative analysis of bone volume/tissue volume (BV/TV), trabecular number (Tb.N), trabecular thickness (Tb.Th), trabecular space (Tb.Sp), and cortical thickness (Cort.Th). *, *p* < 0.05 (versus WT); *n* = 4.

that FBLP-1 deficiency does not impair the formation of mesenchymal stem cells, which can develop into OBs, adipocytes, chondrocytes, and other cell types under distinct conditions. To determine whether a lack of FBLP-1 impacts the formation of OB progenitors from the mesenchymal stem cells, we performed CFU-OB assays using bone marrow cells. The results revealed that the number of CFU-OBs was significantly reduced in *FBLIM1*^{-/-} versus WT bone marrow (Fig. 4, *C* and *D*). Because each colony is derived from a single OB progenitor, the number of CFU-OB colonies reflects the number of mesenchymal progenitors present in the original bone marrow isolates that are capable of differentiating into OBs. These results suggest that lack of FBLP-1 impairs the formation of OB progenitors in bone marrow. This reduction in CFU-OBs could result from impaired cell growth, survival, and/or OB differentiation. To differentiate these possibilities, we performed three sets of experiments. First, MTS assays showed that the growth of *FBLIM1*^{-/-} BMSCs was significantly slower than that of WT BMSCs in cultures at days 2, 4, and 6 (Fig. 4*E*). Second, results from TUNEL staining showed that a loss of FBLP-1 significantly increased the percentage of apoptotic cells in *FBLIM1*^{-/-} versus WT BMSC cultures (Fig. 4, *F* and *G*). Third, we determined whether ablation of the *FBLIM1* gene impacts OB differentiation *in vivo*. We analyzed the expression of Osterix (Osx) protein, a critical transcription factor for OB differentiation, by performing immunohistochemical staining of tibial sections from both genotypes. The numbers of Osx-positive cells (*i.e.*, differentiating and differentiated OBs) located on trabecular bone surfaces were counted and normalized to trabecular bone perimeter (Osx (+) Ob.nb/BPm). Osx-positive OBs were identified on all surfaces throughout the trabeculae of WT tibia. Importantly, Osx (+) Ob.nb/BPm was significantly decreased in *FBLIM1*^{-/-} tibiae compared with that in WT tibiae (Fig. 4, *H* and *I*). In addition, the relative intensity of Osx signal per OB was markedly reduced in *FBLIM1*^{-/-} OBs rela-

tive to WT OBs (Fig. 4*H*). Consistent with the immunohistochemical results, quantitative real time RT-PCR analysis confirmed that the level of *Osx* mRNA was significantly decreased in *FBLIM1*^{-/-} tibiae relative to that of WT tibiae (Fig. 4*J*). These results, together with those described earlier (Fig. 3), demonstrate that inactivation of the *FBLIM1* gene compromises OB behavior *in vitro* as well as in bone.

Deletion of FBLP-1 Increases OCL Differentiation in Vivo—Bone remodeling is controlled by not only OBs/BMSCs but also OCLs. Thus, to better understand the functions of FBLP-1 in bone remodeling, we have analyzed the role of FBLP-1 in OCL differentiation. We first tested whether FBLP-1 deficiency alters OCL differentiation *in vivo*. To do this, the tibiae of 3-month-old WT and *FBLIM1*^{-/-} male mice were fixed, decalcified, and paraffin-embedded, and histological sections were stained for the OCL enzyme tartrate-resistant acid phosphatase (TRAP). The results showed that TRAP activity throughout the tibiae was dramatically increased in *FBLIM1*^{-/-} mice compared with WT mice (Fig. 5*A*). We further measured the effect of FBLP-1 deficiency on OCL differentiation in both primary and secondary spongiosa. The results show that OCL surface/bone surface and OCL number/bone perimeter were significantly increased in both primary and secondary spongiosa in *FBLIM1*^{-/-} tibiae relative to WT tibiae (Fig. 5, *B* and *C*) (*p* < 0.01, WT versus KO). Thus, FBLP-1 deficiency dramatically increases OCL differentiation *in vivo*.

Deletion of FBLP-1 Promotes OCL Differentiation Indirectly by Increasing RANKL Expression in OBs/BMSCs—We next determined whether FBLP-1 is intrinsically required in BMMs for control of OCL differentiation. To do this, we assessed whether or not OCL differentiation was normal upon the addition of exogenous RANKL to *FBLIM1*^{-/-} BMM cultures *in vitro* compared with WT BMM cultures by measuring the numbers of TRAP-positive MNCs generated by each. The results showed that TRAP-positive MNCs (≥3 nuclei/cell)

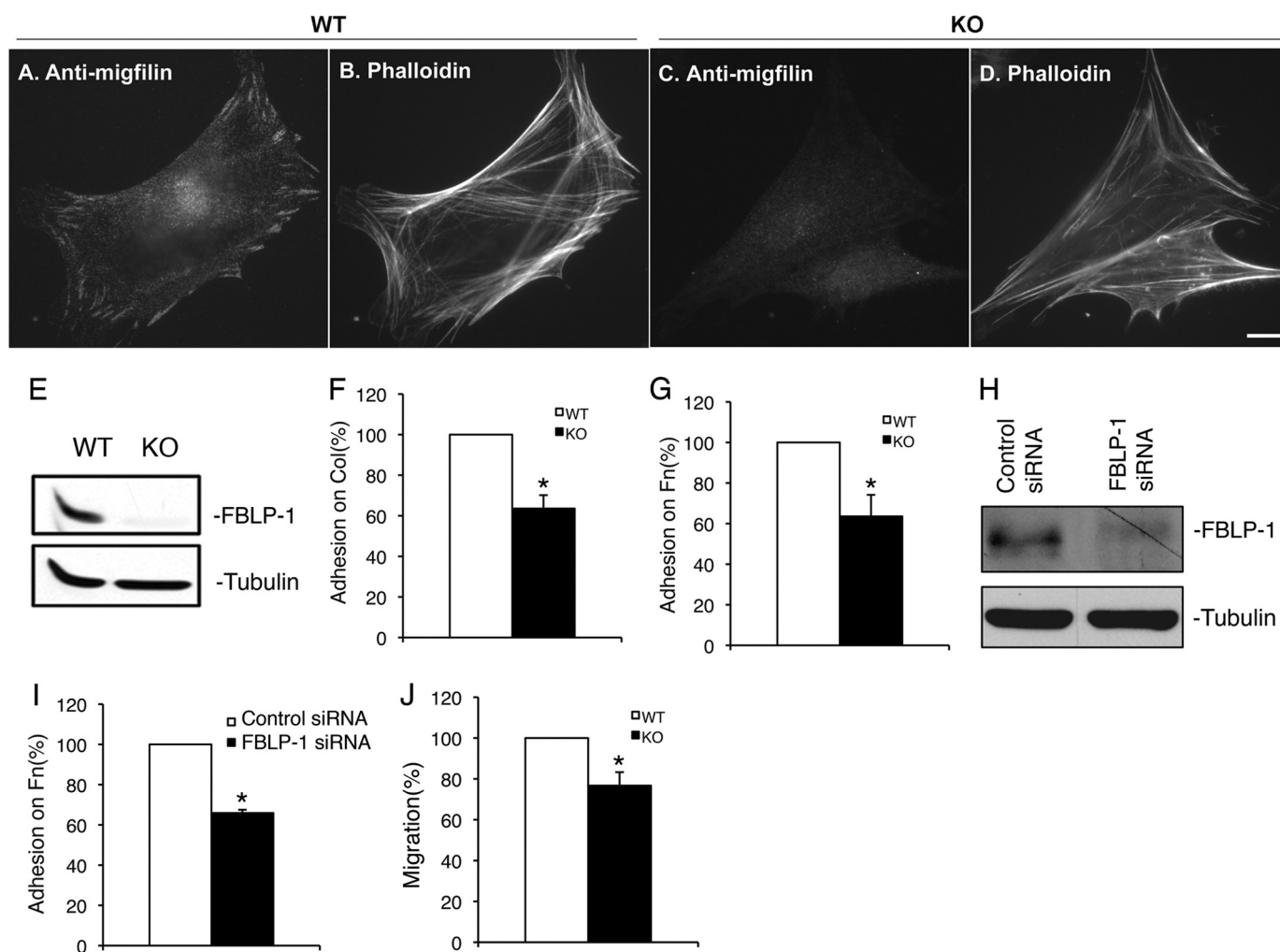


FIGURE 3. Loss of FBLP-1 compromises BMSC-ECM adhesion and migration. *A–D*, primary BMSCs isolated from WT (*A* and *B*) and *FBLIM1*^{-/-} (*C* and *D*) mice were plated on collagen I-coated coverslips and stained with monoclonal anti-FBLP-1 antibody (*A* and *C*) or phalloidin (*B* and *D*). *Bar*, 10 μ m. *E*, primary BMSCs isolated from WT and *FBLIM1*^{-/-} mice were analyzed by Western blotting with antibodies recognizing FBLP-1 or tubulin (as a loading control). *F* and *G*, BMSC-ECM adhesion. Primary BMSCs isolated from WT and *FBLIM1*^{-/-} mice were plated in type I collagen-coated (*F*) or fibronectin-coated (*G*) 96-well plates and incubated at 37 °C for 15 min. Cell-ECM adhesion was analyzed using a quantitative centrifugal force assay as described under “Experimental Procedures.” Adhesion of *FBLIM1*^{-/-} BMSCs was compared with that of WT BMSCs (normalized to 100%). The *bars* represent the means \pm S.D. from three independent experiments. *, $p < 0.05$ (versus WT). *H* and *I*, MC4 cell-ECM adhesion. MC4 cells were transfected with FBLP-1 or control siRNA. The FBLP-1 siRNA and control transfectants were analyzed by Western blotting with antibodies recognizing FBLP-1 or tubulin (*H*) or a quantitative centrifugal force cell-ECM adhesion assay (*I*). Adhesion of FBLP-1 knockdown MC4 cells was compared with that of control MC4 cells (normalized to 100%). The *bars* in *I* represent the means \pm S.D. from three independent experiments. *, $p < 0.05$ (versus control). *J*, cell migration was assessed with a scratch assay as described under “Experimental Procedures.” The distances traveled by *FBLIM1*^{-/-} BMSCs at the acellular fronts were measured 6.5 h after wounding and compared with those of WT BMSCs (normalized to 100%). The *bars* represent the means \pm S.D. from three independent experiments. *, $p < 0.05$ (versus WT).

were not significantly different in BMM cultures of the two genotypes (Fig. 6, *A* and *B*). Thus, a lack of FBLP-1 does not increase the capacity of BMMs to differentiate into multinucleated OCLs in response to exogenously supplied RANKL. This result prompted us to determine whether a lack of FBLP-1 increases the ability of BMSCs, which are the main source of endogenous RANKL, to promote OCL differentiation in BMMs. To do this, BMMs and BMSCs from WT or *FBLIM1*^{-/-} mice were cocultured in the absence of exogenously supplied RANKL. As expected, cocultures of WT BMSCs with WT BMMs induced the formation of TRAP-positive MNCs. However, the number of TRAP-positive MNCs formed from the *FBLIM1*^{-/-}-BMSC/*FBLIM1*^{-/-}-BMM cocultures was dramatically increased compared with that formed from the WT-BMSC/WT-BMM cocultures (WT-BMSC/WT-BMM: $1.5 \pm$

2.0 MNC/10 \times field, *FBLIM1*^{-/-}-BMSC/*FBLIM1*^{-/-}-BMM: 7.5 ± 6.0 MNC/10 \times field, $p = 0.002$) (Fig. 6*C*). Furthermore, the number of nuclei per MNC was significantly increased in *FBLIM1*^{-/-}-BMSC/*FBLIM1*^{-/-}-BMM cocultures compared with WT-BMSC/WT-BMM cocultures (WT-BMSC/WT-BMM: 4.2 ± 1.3 , *FBLIM1*^{-/-}-BMSC/*FBLIM1*^{-/-}-BMM: 13.7 ± 14.8 , $p = 0.018$), and the MNCs that formed in the *FBLIM1*^{-/-}-BMSC/*FBLIM1*^{-/-}-BMM cocultures were strikingly larger than those formed in the WT-BMSC/WT-BMM cocultures (Fig. 6*C*). These results, together with those shown in Fig. 6 (*A* and *B*), suggest that FBLP-1 deficiency may promote OCL differentiation via up-regulation of RANKL expression in OBs/BMSCs. To test this experimentally, we measured the level of *Rankl* mRNA in primary BMSCs from WT and *FBLIM1*^{-/-} mice. The results showed that the level of *Rankl*

FBLP-1 in Bone Remodeling

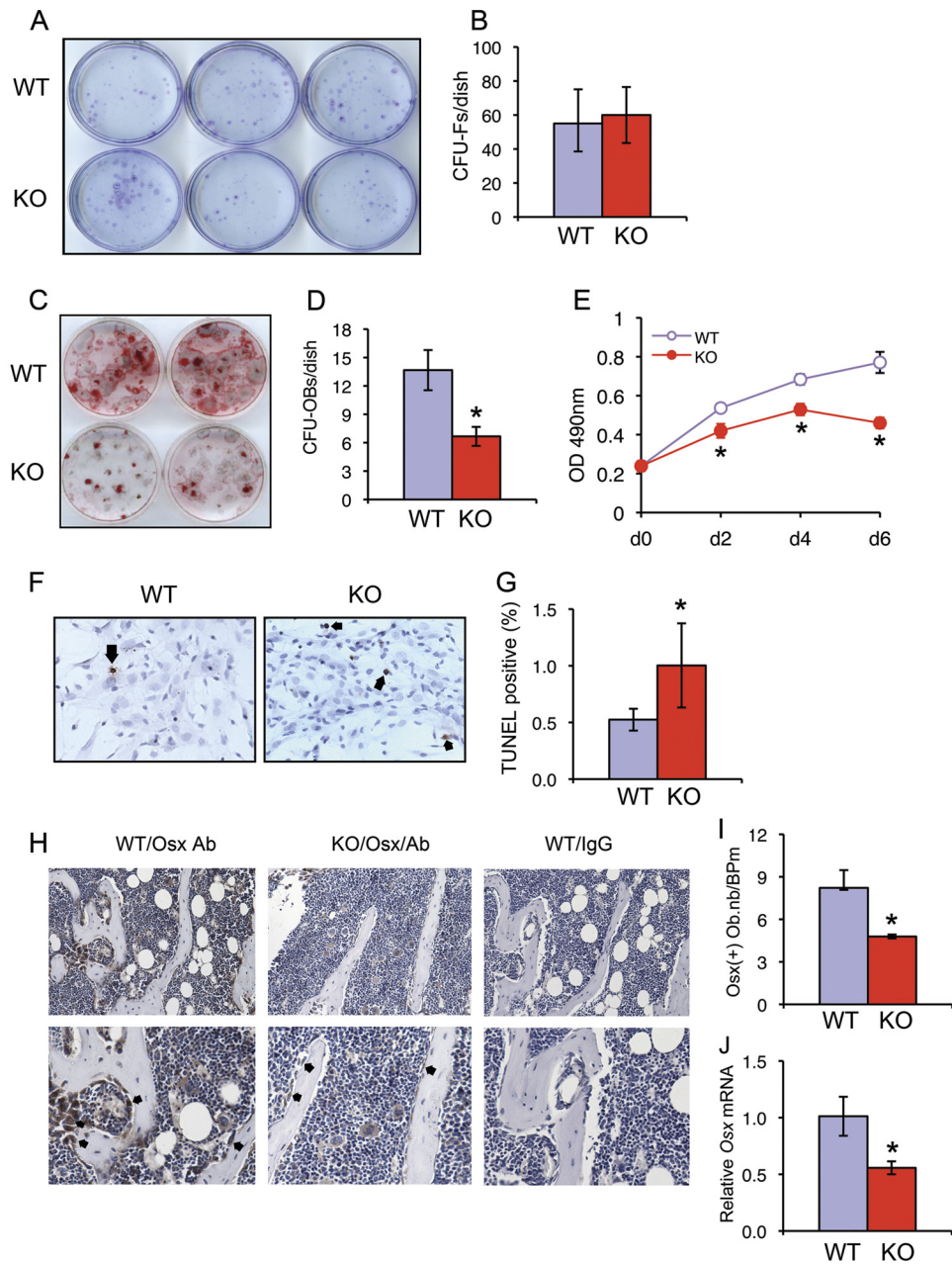


FIGURE 4. FBLP-1 ablation compromises the formation of OB progenitors in bone marrow and OB differentiation *in vivo*. A and B, CFU-F assay. 1×10^6 bone marrow-nucleated cells from WT and *FBLIM1*^{-/-} mice were cultured for 10 days, and CFU-Fs were quantified as described under “Experimental Procedures.” The bars in B represent the means \pm S.D. from three experiments. C and D, CFU-OB assay. 1×10^6 bone marrow-nucleated cells from WT and *FBLIM1*^{-/-} mice were cultured in OB differentiation medium for 21 days, and the numbers of CFU-OB colonies were quantified as described under “Experimental Procedures.” The bars in D represent the means \pm S.D. from four experiments. *, $p < 0.05$ (versus WT). E, BMSC growth. WT and *FBLIM1*^{-/-} BMSCs were seeded at a density of 1×10^4 /well in 96-well plates in proliferation medium. MTS assays were performed on days 0, 2, 4, and 6 (*d0*, *d2*, *d4*, and *d6*, respectively) as indicated. *, $p < 0.05$ (versus WT). F and G, TUNEL staining. Apoptosis of WT and *FBLIM1*^{-/-} BMSCs was analyzed by TUNEL staining as described under “Experimental Procedures.” The arrows in F indicate TUNEL-positive cells. The bars in G represent the means \pm S.D. from five experiments. *, $p < 0.05$ (versus WT). H and I, Osx staining. Five- μ m tibial sections from 3-month-old WT and *FBLIM1*^{-/-} male mice were immunohistochemically stained with anti-Osx antibody or control IgG as indicated in H. The arrows in H indicate the nuclei of Osx-positive OBs that were stained brown. Osx-negative cells were stained blue. Original magnification was $\times 100$ (top) and $\times 200$ (bottom). I, the numbers of Osx-positive cells (*i.e.*, differentiating and differentiated OBs) located on trabecular bone surfaces were counted and normalized to trabecular bone perimeter (Osx (+) Ob.nb/BPm) using an Image Pro Plus 6.2 software. *, $p < 0.05$ (versus WT); $n = 4$. J, real time RT-PCR. Tibiae from 2-month-old WT and *FBLIM1*^{-/-} mice ($n = 4$) were harvested for RNA isolation. Total RNA was used for quantitative real time PCR using specific primers for *Osx* mRNAs, which were normalized to *GAPDH* mRNA. *, $p < 0.05$ (versus WT); $n = 4$.

mRNA was indeed dramatically increased in *FBLIM1*^{-/-} BMSCs compared with that in WT cells (Fig. 6D). By contrast, the level of *Opg* mRNA was not significantly altered by the lack of FBLP-1 in BMSCs (Fig. 6D). Western blot analysis confirmed that the level of RANKL protein was markedly increased in *FBLIM1*^{-/-} versus WT BMSCs (Fig. 6E). Consistent with the

results from the *in vitro* studies (Fig. 6, D and E), immunohistochemical staining of tibial sections using specific antibody for RANKL or normal IgG as a control showed that the level of RANKL was markedly increased in OBs of *FBLIM1*^{-/-} tibiae compared with that of WT tibiae (Fig. 6F). Taken together, these results suggest that a loss of FBLP-1 increases the expres-

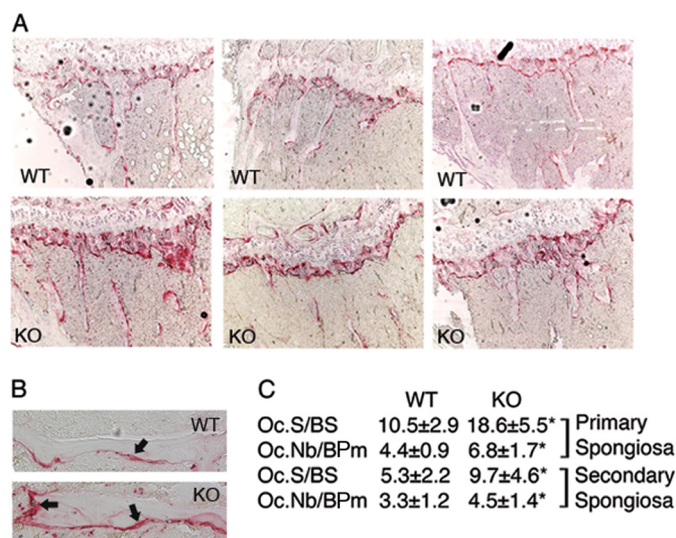


FIGURE 5. FBLP-1 deficiency dramatically increases OCL differentiation *in vivo*. *A*, TRAP staining. Tibial sections of 3-month-old WT and *FBLP1*^{-/-} male mice were stained for TRAP activity for 30 min at 37 °C. *B*, TRAP activity in metaphyseal regions of tibiae is shown. The arrows indicate TRAP-positive MNCs on trabecular surfaces. *C*, OCL surface/bone surface (*Oc.S/BS*) and OCL number/bone perimeter (*Oc.Nb/BPm*) in both primary and secondary spongiosa of tibiae in *A* were measured as described previously (33). *, *p* < 0.05 (versus WT); *n* = 4

sion of RANKL in OBs/BMSCs and consequently promotes OCL differentiation *in vivo*.

Loss of FBLP-1 Up-regulates RANKL Expression via Promoting ERK1/2 Activation—RANKL expression can be regulated by ERK1/2 or AKT signaling pathways (48–51). To test how loss of FBLP-1 promotes RANKL expression in BMSCs, we analyzed the levels of ERK1/2, phospho-ERK1/2, AKT, and phospho-AKT in *FBLP1*^{-/-} and WT BMSCs. The results showed that loss of FBLP-1 did not alter the total protein levels of ERK1/2 (Fig. 7A). However, the level of the activating phosphorylation of ERK1/2 was dramatically increased in *FBLP1*^{-/-} BMSCs compared with that in WT BMSCs (Fig. 7A). By contrast, no significant change of the protein level or activating phosphorylation of AKT was detected in response to a loss of FBLP-1 (Fig. 7A). These results suggest that a loss of FBLP-1 probably increases RANKL expression via promoting ERK activation. To test this experimentally, we suppressed ERK1/2 activation with UO126 and found that this effectively blocked the up-regulation of RANKL expression induced by the loss of FBLP-1 (Fig. 7B). Collectively, these results strongly suggest that FBLP-1 deficiency decreases bone mass via, at least in part, up-regulation of ERK1/2 activation and RANKL expression in OBs/BMSCs, resulting in increased OCL differentiation and bone resorption.

DISCUSSION

Bone remodeling is a tightly regulated process whose alteration is a major cause of common human bone diseases including osteoporosis. Recent studies have pointed to an important role for OB/BMSCs-OCL communication in maintaining the balance of bone formation and resorption, but the molecular mechanism that governs this process is incompletely understood. Using a genetic KO approach, we have demonstrated that FBLP-1 is indispensable for maintaining bone homeostasis

in mice. Furthermore, our studies have revealed important roles for FBLP-1 in regulation of OB/BMSC behavior including ECM adhesion, migration, growth, survival, formation of OB progenitors in bone marrow, OB differentiation, and RANKL expression. Additionally, we have found that FBLP-1 functions in maintaining the balance of bone remodeling via regulation not only of intrinsic properties of OBs/BMSCs but also of OB/BMSC-OCL communication that controls osteoclastogenesis. Specifically, we have found that a loss of FBLP-1 results in a dramatic increase of RANKL expression and OCL differentiation *in vivo*, whereas the capacity of OCL differentiation in response to exogenously supplied RANKL was not altered in response to loss of FBLP-1. Because RANKL plays a pivotal role in bone remodeling and pathogenesis of common human bone diseases, we sought to further test the signaling intermediate that links FBLP-1 to RANKL expression. Our results show that a loss of FBLP-1 increases the activation of ERK1/2 but not that of AKT. Furthermore, suppression of ERK1/2 activation effectively reduces the increase of RANKL expression induced by the loss of FBLP-1, validating that the increased activation of ERK1/2 is responsible for, at least in part, the up-regulation of RANKL expression in *FBLP1*^{-/-} BMSCs.

When the current study was in progress, Moik *et al.* (52) reported that a loss of FBLP-1 expression permits normal embryonic development in mice. Bone or bone cells, however, were not analyzed in the study by Moik *et al.* (52). Interestingly, Moik *et al.* (52) observed different effects of loss of FBLP-1 on the two cell types (embryonic fibroblasts and keratinocytes) that they have analyzed; loss of FBLP-1 causes a migratory defect in keratinocytes but not embryonic fibroblasts. Thus, the functions of FBLP-1 appear to be cell- and tissue context-dependent. The severe osteopenic phenotype discovered in the current study reveals a particularly important role of FBLP-1 in bone. Although our studies have clearly demonstrated important roles of FBLP-1 in regulation of OB/BMSC behavior including ECM adhesion, migration, BMSC growth, survival, OB formation, differentiation, and RANKL expression, we cannot exclude the possibility that FBLP-1 may also play a role in other bone cell types, although the capacity of *FBLP1*^{-/-} BMMs to differentiate into multinucleated OCLs in response to exogenously supplied RANKL appears to be normal.

FBLP-1 possesses multiple protein binding activities but no catalytic activities (15, 21–22, 27). Thus, the strong dependence of healthy bone on FBLP-1 likely reflects a critical role for one or multiple FBLP-1-mediated interactions in this organ that is undergoing continuous cycles of remodeling. In this regard, it is worth noting that kindlin-2 and filamin, which directly bind FBLP-1 (15), have been implicated in regulation of bone remodeling. For example, Brunner *et al.* (53) recently showed that kindlin-2 plays an important role in regulation of OB behavior. Hence, the interaction of FBLP-1 with kindlin-2 could contribute to, at least in part, FBLP-1-mediated regulation of bone remodeling. Numerous genetic and biochemical studies have also pointed to a critical role of filamin in bone. For example, mutations in genes encoding filamin have been associated with human genetic diseases with defects in bone (54). Furthermore, loss or mutation in genes encoding filamin A or B in mice also cause dramatic bone phenotypes including skeletal dysplasia or

FBLP-1 in Bone Remodeling

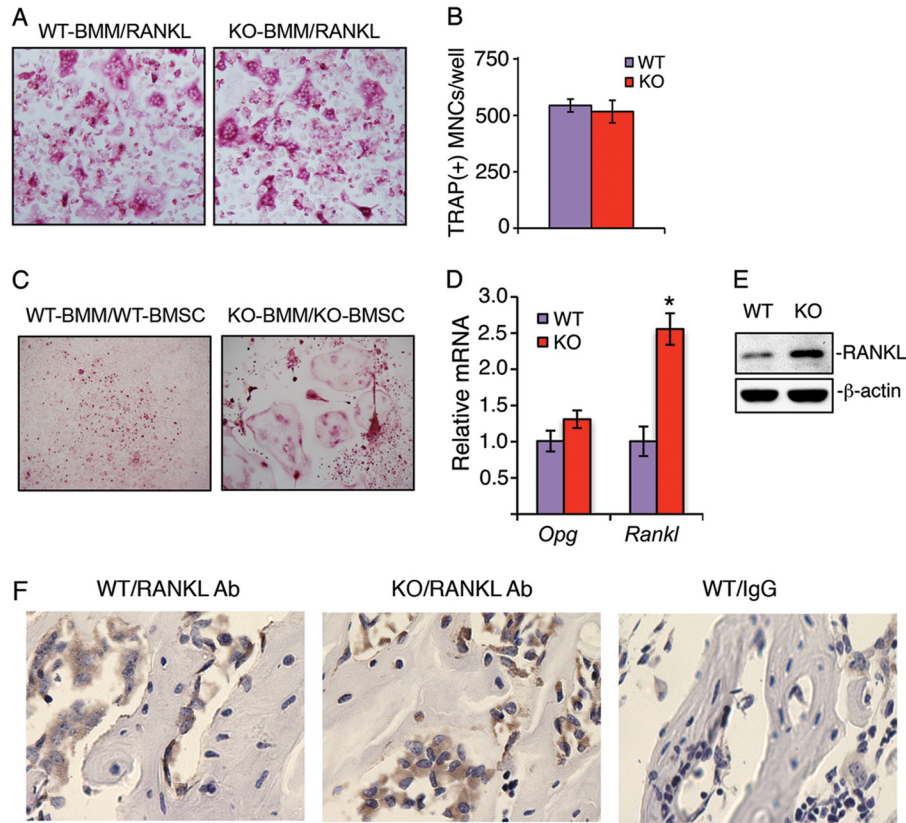


FIGURE 6. Loss of FBLP-1 promotes OCL differentiation via up-regulation of RANKL expression in OBs/BMSCs. *A* and *B*, TRAP staining. WT and *FBLIM1*^{-/-} BMM differentiation were induced with M-CSF (10 ng/ml) and RANKL (50 ng/ml) for 7 days, followed by TRAP staining (*A*). TRAP-positive MNCs (three or more nuclei) per well were scored (*B*). *C*, BMSC-BMM coculture. Primary BMSCs and BMMs from 2-month-old WT and *FBLIM1*^{-/-} mice were cocultured in the absence of exogenously supplied RANKL for 10 days, followed by TRAP staining. *D* and *E*, real time RT-PCR and Western blot. Primary BMSCs from 2-month-old WT and *FBLIM1*^{-/-} mice were seeded at a density of $5 \times 10^4/\text{cm}^2$ in 35-mm dish in proliferation medium for 24 h and harvested for RNA and protein isolation. Total RNA was used for quantitative real time PCR (*D*) using specific primers for *Rankl* and *Opg* mRNAs, which were normalized to *GAPDH* mRNA. Whole cell extracts were used for Western blot with antibodies as specified in the figure (*E*). *F*, immunohistochemical staining. Five- μm tibial sections from 3-month-old WT and *FBLIM1*^{-/-} male mice were immunohistochemically stained with anti-RANKL antibody or control IgG as indicated in the figure.

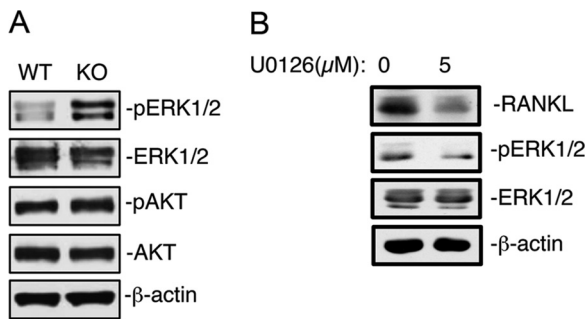


FIGURE 7. Loss of FBLP-1 increases RANKL expression via promoting ERK1/2 activation in BMSCs. *A*, loss of FBLP-1 promotes activating phosphorylation of ERK1/2. Primary BMSCs from 2-month-old WT and *FBLIM1*^{-/-} mice were seeded at a density of $5 \times 10^4/\text{cm}^2$ in 35-mm dish in proliferation medium for 24 h and harvested for protein isolation and Western blot with antibodies against phospho-ERK1/2 (Thr-202/Tyr-204), ERK1/2, phospho-AKT (Ser-473), AKT, and β -actin as indicated in the figure. *B*, inhibition of ERK1/2 activation suppresses FBLP-1 deficiency induced RANKL expression. Primary BMSCs from 2-month-old *FBLIM1*^{-/-} mice were seeded at a density of $5 \times 10^4/\text{cm}^2$ in 35-mm dish in proliferation medium for 24 h and treated with and without U0126 (5 μM) for 24 h, followed by Western blotting with antibodies against RANKL, phospho-ERK1/2 (Thr-202/Tyr-204), ERK1/2, and β -actin as indicated in the figure.

reduced bone mineral density (55, 56). Finally, filamin A can directly interact with Runx2, a master regulator of OB differentiation and bone formation, and regulate Runx2-mediated gene expression in these cells (57). Thus, it is conceivable that

FBLP-1 may work in concert with its binding partners kindlin-2 and filamin in bone. Future studies are required to define the role of each of these interactions in bone, which may lead to novel strategies to battle human diseases associated with abnormal bone remodeling. Clearly, the findings presented in this communication will greatly facilitate the design and execution of future studies.

Acknowledgments—We thank Kenneth Patrene (University of Pittsburgh) for technical support on the microcomputerized tomography analysis of bone.

REFERENCES

- Ash, P., Loutit, J. F., and Townsend, K. M. (1980) Osteoclasts derived from haematopoietic stem cells. *Nature* **283**, 669–670
- Lacey, D. L., Timms, E., Tan, H. L., Kelley, M. J., Dunstan, C. R., Burgess, T., Elliott, R., Colombero, A., Elliott, G., Scully, S., Hsu, H., Sullivan, J., Hawkins, N., Davy, E., Capparelli, C., Eli, A., Qian, Y. X., Kaufman, S., Sarosi, I., Shalhoub, V., Senaldi, G., Guo, J., Delaney, J., and Boyle, W. J. (1998) Osteoprotegerin ligand is a cytokine that regulates osteoclast differentiation and activation. *Cell* **93**, 165–176
- Yasuda, H., Shima, N., Nakagawa, N., Yamaguchi, K., Kinoshita, M., Mochizuki, S., Tomoyasu, A., Yano, K., Goto, M., Murakami, A., Tsuda, E., Morinaga, T., Higashio, K., Udagawa, N., Takahashi, N., and Suda, T. (1998) Osteoclast differentiation factor is a ligand for osteoprotegerin/osteoclastogenesis-inhibitory factor and is identical to TRANCE/RANKL.

- Proc. Natl. Acad. Sci. U.S.A.* **95**, 3597–3602
4. Simonet, W. S., Lacey, D. L., Dunstan, C. R., Kelley, M., Chang, M. S., Lüthy, R., Nguyen, H. Q., Woodson, S., Bennett, L., Boone, T., Shimamoto, G., DeRose, M., Elliott, R., Colombero, A., Tan, H. L., Trail, G., Sullivan, J., Davy, E., Bucay, N., Renshaw-Gegg, L., Hughes, T. M., Hill, D., Pattison, W., Campbell, P., Sander, S., Van, G., Tarpley, J., Derby, P., Lee, R., and Boyle, W. J. (1997) Osteoprotegerin. A novel secreted protein involved in the regulation of bone density. *Cell* **89**, 309–319
 5. O'Brien, C. A. (2010) Control of RANKL gene expression. *Bone* **46**, 911–919
 6. Boyle, W. J., Simonet, W. S., and Lacey, D. L. (2003) Osteoclast differentiation and activation. *Nature* **423**, 337–342
 7. Asagiri, M., and Takayanagi, H. (2007) The molecular understanding of osteoclast differentiation. *Bone* **40**, 251–264
 8. Yavropoulou, M. P., and Yovos, J. G. (2008) Osteoclastogenesis. Current knowledge and future perspectives. *J. Musculoskelet. Neuronal Interact.* **8**, 204–216
 9. Roodman, G. D., and Windle, J. J. (2005) Paget disease of bone. *J. Clin. Invest.* **115**, 200–208
 10. Matsuo, K., and Irie, N. (2008) Osteoclast-osteoblast communication. *Arch. Biochem. Biophys.* **473**, 201–209
 11. Sims, N. A., and Gooi, J. H. (2008) Bone remodeling. Multiple cellular interactions required for coupling of bone formation and resorption. *Semin. Cell Dev. Biol.* **19**, 444–451
 12. Henriksen, K., Neutsky-Wulff, A. V., Bonewald, L. F., and Karsdal, M. A. (2009) Local communication on and within bone controls bone remodeling. *Bone* **44**, 1026–1033
 13. Nakahama, K. (2010) Cellular communications in bone homeostasis and repair. *Cell Mol. Life Sci.* **67**, 4001–4009
 14. Cao, X. (2011) Targeting osteoclast-osteoblast communication. *Nat. Med.* **17**, 1344–1346
 15. Tu, Y., Wu, S., Shi, X., Chen, K., and Wu, C. (2003) Migfilin and Mig-2 link focal adhesions to filamin and the actin cytoskeleton and function in cell shape modulation. *Cell* **113**, 37–47
 16. Larjava, H., Plow, E. F., and Wu, C. (2008) Kindlins. Essential regulators of integrin signalling and cell-matrix adhesion. *EMBO Rep.* **9**, 1203–1208
 17. Meves, A., Stremmel, C., Gottschalk, K., and Fässler, R. (2009) The Kindlin protein family. New members to the club of focal adhesion proteins. *Trends Cell Biol.* **19**, 504–513
 18. Moser, M., Legate, K. R., Zent, R., and Fässler, R. (2009) The tail of integrins, talin, and kindlins. *Science* **324**, 895–899
 19. Plow, E. F., Qin, J., and Byzova, T. (2009) Kindling the flame of integrin activation and function with kindlins. *Curr. Opin. Hematol.* **16**, 323–328
 20. Lai-Cheong, J. E., Parsons, M., and McGrath, J. A. (2010) The role of kindlins in cell biology and relevance to human disease. *Int. J. Biochem. Cell Biol.* **42**, 595–603
 21. Wu, C. (2005) Migfilin and its binding partners. From cell biology to human diseases. *J. Cell Sci.* **118**, 659–664
 22. Zhang, Y., Tu, Y., Gkretsi, V., and Wu, C. (2006) Migfilin interacts with vasodilator-stimulated phosphoprotein (VASP) and regulates VASP localization to cell-matrix adhesions and migration. *J. Biol. Chem.* **281**, 12397–12407
 23. Gkretsi, V., Zhang, Y., Tu, Y., Chen, K., Stolz, D. B., Yang, Y., Watkins, S. C., and Wu, C. (2005) Physical and functional association of migfilin with cell-cell adhesions. *J. Cell Sci.* **118**, 697–710
 24. Lad, Y., Jiang, P., Ruskamo, S., Harburger, D. S., Ylänen, J., Campbell, I. D., and Calderwood, D. A. (2008) Structural basis of the migfilin-filamin interaction and competition with integrin β tails. *J. Biol. Chem.* **283**, 35154–35163
 25. Lai-Cheong, J. E., Ussar, S., Arita, K., Hart, I. R., and McGrath, J. A. (2008) Colocalization of kindlin-1, kindlin-2, and migfilin at keratinocyte focal adhesion and relevance to the pathophysiology of Kindler syndrome. *J. Invest. Dermatol.* **128**, 2156–2165
 26. Ithychanda, S. S., Das, M., Ma, Y. Q., Ding, K., Wang, X., Gupta, S., Wu, C., Plow, E. F., and Qin, J. (2009) Migfilin, a molecular switch in regulation of integrin activation. *J. Biol. Chem.* **284**, 4713–4722
 27. Zhao, J., Zhang, Y., Ithychanda, S. S., Tu, Y., Chen, K., Qin, J., and Wu, C. (2009) Migfilin interacts with Src and contributes to cell-matrix adhesion-mediated survival signaling. *J. Biol. Chem.* **284**, 34308–34320
 28. Das, M., Ithychanda, S. S., Qin, J., and Plow, E. F. (2011) Migfilin and filamin as regulators of integrin activation in endothelial cells and neutrophils. *PLoS One* **6**, e26355
 29. Ithychanda, S. S., and Qin, J. (2011) Evidence for multisite ligand binding and stretching of filamin by integrin and migfilin. *Biochemistry* **50**, 4229–4231
 30. Liang, X., Zhou, Q., Li, X., Sun, Y., Lu, M., Dalton, N., Ross, J., Jr., and Chen, J. (2005) PINCH1 plays an essential role in early murine embryonic development but is dispensable in ventricular cardiomyocytes. *Mol. Cell. Biol.* **25**, 3056–3062
 31. Cheng, H., Kimura, K., Peter, A. K., Cui, L., Ouyang, K., Shen, T., Liu, Y., Gu, Y., Dalton, N. D., Evans, S. M., Knowlton, K. U., Peterson, K. L., and Chen, J. (2010) Loss of enigma homolog protein results in dilated cardiomyopathy. *Circ. Res.* **107**, 348–356
 32. O'Gorman, S., Dagenais, N. A., Qian, M., and Marchuk, Y. (1997) Protamine-Cre recombinase transgenes efficiently recombine target sequences in the male germ line of mice, but not in embryonic stem cells. *Proc. Natl. Acad. Sci. U.S.A.* **94**, 14602–14607
 33. Cao, H., Yu, S., Yao, Z., Galson, D. L., Jiang, Y., Zhang, X., Fan, J., Lu, B., Guan, Y., Luo, M., Lai, Y., Zhu, Y., Kurihara, N., Patrene, K., Roodman, G. D., and Xiao, G. (2010) Activating transcription factor 4 regulates osteoclast differentiation in mice. *J. Clin. Invest.* **120**, 2755–2766
 34. Yu, S., Franceschi, R. T., Luo, M., Fan, J., Jiang, D., Cao, H., Kwon, T. G., Lai, Y., Zhang, J., Patrene, K., Hankenson, K., Roodman, G. D., and Xiao, G. (2009) Critical role of activating transcription factor 4 in the anabolic actions of parathyroid hormone in bone. *PLoS One* **4**, e7583
 35. Yu, S., Franceschi, R. T., Luo, M., Zhang, X., Jiang, D., Lai, Y., Jiang, Y., Zhang, J., and Xiao, G. (2008) Parathyroid hormone increases activating transcription factor 4 expression and activity in osteoblasts. Requirement for osteocalcin gene expression. *Endocrinology* **149**, 1960–1968
 36. Yu, S., Jiang, Y., Galson, D. L., Luo, M., Lai, Y., Lu, Y., Ouyang, H. J., Zhang, J., and Xiao, G. (2008) General transcription factor IIA- γ increases osteoblast-specific osteocalcin gene expression via activating transcription factor 4 and runt-related transcription factor 2. *J. Biol. Chem.* **283**, 5542–5553
 37. Xiao, G., Jiang, D., Gopalakrishnan, R., and Franceschi, R. T. (2002) Fibroblast growth factor 2 induction of the osteocalcin gene requires MAPK activity and phosphorylation of the osteoblast transcription factor, Cbfa1/Runx2. *J. Biol. Chem.* **277**, 36181–36187
 38. Qu, H., Tu, Y., Shi, X., Larjava, H., Saleem, M. A., Shattil, S. J., Fukuda, K., Qin, J., Kretzler, M., and Wu, C. (2011) Kindlin-2 regulates podocyte adhesion and fibronectin matrix deposition through interactions with phosphoinositides and integrins. *J. Cell Sci.* **124**, 879–891
 39. Shi, X., Ma, Y. Q., Tu, Y., Chen, K., Wu, S., Fukuda, K., Qin, J., Plow, E. F., and Wu, C. (2007) The MIG-2/integrin interaction strengthens cell-matrix adhesion and modulates cell motility. *J. Biol. Chem.* **282**, 20455–20466
 40. Zhang, Y., Guo, L., Chen, K., and Wu, C. (2002) A critical role of the PINCH-integrin-linked kinase interaction in the regulation of cell shape change and migration. *J. Biol. Chem.* **277**, 318–326
 41. Xiao, G., Cui, Y., Ducey, P., Karsenty, G., and Franceschi, R. T. (1997) Ascorbic acid-dependent activation of the osteocalcin promoter in MC3T3-E1 preosteoblasts. Requirement for collagen matrix synthesis and the presence of an intact OSE2 sequence. *Mol. Endocrinol.* **11**, 1103–1113
 42. Singha, U. K., Jiang, Y., Yu, S., Luo, M., Lu, Y., Zhang, J., and Xiao, G. (2008) Rapamycin inhibits osteoblast proliferation and differentiation in MC3T3-E1 cells and primary mouse bone marrow stromal cells. *J. Cell. Biochem.* **103**, 434–446
 43. Termine, J. D. (1990) Cellular activity, matrix proteins, and aging bone. *Exp. Gerontol.* **25**, 217–221
 44. Moursi, A. M., Damsky, C. H., Lull, J., Zimmerman, D., Doty, S. B., Aota, S., and Globus, R. K. (1996) Fibronectin regulates calvarial osteoblast differentiation. *J. Cell Sci.* **109**, 1369–1380
 45. Marini, J. C., Forlino, A., Cabral, W. A., Barnes, A. M., San Antonio, J. D., Milgrom, S., Hyland, J. C., Körkkö, J., Prockop, D. J., De Paepe, A., Coucke, P., Symoens, S., Glorieux, F. H., Roughley, P. J., Lund, A. M., Kuurila-Svahn, K., Hartikka, H., Cohn, D. H., Krakow, D., Mottes, M., Schwarze,

- U., Chen, D., Yang, K., Kuslich, C., Troendle, J., Dalglish, R., and Byers, P. H. (2007) Consortium for osteogenesis imperfecta mutations in the helical domain of type I collagen. Regions rich in lethal mutations align with collagen binding sites for integrins and proteoglycans. *Hum. Mutat.* **28**, 209–221
46. Shekaran, A., and García, A. J. (2011) Extracellular matrix-mimetic adhesive biomaterials for bone repair. *J. Biomed. Mater. Res. A* **96**, 261–272
47. Siebers, M. C., ter Brugge, P. J., Walboomers, X. F., and Jansen, J. A. (2005) Integrins as linker proteins between osteoblasts and bone replacing materials. A critical review. *Biomaterials* **26**, 137–146
48. Nishida, S., Tsubaki, M., Hoshino, M., Namimatsu, A., Uji, H., Yoshioka, S., Tanimori, Y., Yanae, M., Iwaki, M., and Irimajiri, K. (2005) Nitrogen-containing bisphosphonate, YM529/ONO-5920 (a novel minodronic acid), inhibits RANKL expression in a cultured bone marrow stromal cell line ST2. *Biochem. Biophys. Res. Commun.* **328**, 91–97
49. Matsushita, T., Chan, Y. Y., Kawanami, A., Balmes, G., Landreth, G. E., and Murakami, S. (2009) Extracellular signal-regulated kinase 1 (ERK1) and ERK2 play essential roles in osteoblast differentiation and in supporting osteoclastogenesis. *Mol. Cell. Biol.* **29**, 5843–5857
50. Walker, C. G., Dangaria, S., Ito, Y., Luan, X., and Diekwisch, T. G. (2010) Osteopontin is required for unloading-induced osteoclast recruitment and modulation of RANKL expression during tooth drift-associated bone remodeling, but not for super-eruption. *Bone* **47**, 1020–1029
51. Lee, J. H., Kim, H. N., Yang, D., Jung, K., Kim, H. M., Kim, H. H., Ha, H., and Lee, Z. H. (2009) Trolox prevents osteoclastogenesis by suppressing RANKL expression and signaling. *J. Biol. Chem.* **284**, 13725–13734
52. Moik, D. V., Janbandhu, V. C., and Fässler, R. (2011) Loss of migfilin expression has no overt consequences on murine development and homeostasis. *J. Cell Sci.* **124**, 414–421
53. Brunner, M., Millon-Frémillon, A., Chevalier, G., Nakchbandi, I. A., Mosher, D., Block, M. R., Albigès-Rizo, C., and Bouvard, D. (2011) Osteoblast mineralization requires β 1 integrin/ICAP-1-dependent fibronectin deposition. *J. Cell Biol.* **194**, 307–322
54. Feng, Y., and Walsh, C. A. (2004) The many faces of filamin. A versatile molecular scaffold for cell motility and signalling. *Nat. Cell Biol.* **6**, 1034–1038
55. Hart, A. W., Morgan, J. E., Schneider, J., West, K., McKie, L., Bhattacharya, S., Jackson, I. J., and Cross, S. H. (2006) Cardiac malformations and midline skeletal defects in mice lacking filamin A. *Hum. Mol. Genet.* **15**, 2457–2467
56. Zhou, X., Tian, F., Sandzén, J., Cao, R., Flaberg, E., Szekely, L., Cao, Y., Ohlsson, C., Bergo, M. O., Borén, J., and Akyürek, L. M. (2007) Filamin B deficiency in mice results in skeletal malformations and impaired microvascular development. *Proc. Natl. Acad. Sci. U.S.A.* **104**, 3919–3924
57. Camacho, C. L. (2011) *A New Role for Filamin A as a Regulator of Runx2 Function*. Doctoral dissertation, University of Manchester, Manchester, UK